

## Radiation-Induced Changes in the Degree of Crystallinity of Powdered Polytetrafluoroethylene

A. S. Smolyanskii<sup>a,b,\*</sup>, M. A. Arsenyev<sup>a</sup>, A. Yu. Rashkovskii<sup>c</sup>, and E. D. Politova<sup>a</sup>

<sup>a</sup> Mendeleev University of Chemical Technology, Moscow, 125047 Russia

<sup>b</sup> Branch of JSC Karpov Institute of Physical Chemistry, Moscow, 105064 Russia

<sup>c</sup> Systems for Microscopy and Analysis Ltd., Moscow, 121353 Russia

\*e-mail: assafci@gmail.com

Received April 12, 2018; revised April 12, 2018; accepted May 21, 2018

**Abstract**—An analysis of the diffraction patterns of powdered polytetrafluoroethylene (PTFE)  $\gamma$ -irradiated at room temperature in a nitrogen atmosphere to doses of 10–500 kGy with a fluence of  $1.50 \pm 0.3$  Gy/s has shown that the diffraction peak 100 of the crystalline phase at  $2\theta \sim 18^\circ$  and the halo at  $2\theta = 10^\circ\text{--}25^\circ$  are most sensitive to ionizing radiation. It is found that the intensity, FWHM, and position of the maximum of reflection 100 change with an increase in the absorbed dose; this fact is indicative of the doublet nature of the peak profile. It is established that the doublet components differently respond to ionizing radiation. The interplanar spacings, amplitude and sign of arising stress, and the degree of crystallinity (DOC) of polymer are calculated as functions of the irradiation dose. The radiation-induced change in the DOC of PTFE should be considered as a complex process, which includes radiative destruction and topochemical reactions of different types in crystals.

DOI: 10.1134/S1063774519040205

### INTRODUCTION

The radiolysis of amorphous–crystalline polymers, including a polymer of practical importance—polytetrafluoroethylene (PTFE) [1], may often cause changes in the degree of crystallinity (DOC) [2]. Crystallites can be grown under PTFE irradiation according to different mechanisms, which are accompanied by the formation of extended defects (dislocations, microcracks, pores) [3–5]; during the PTFE radiolysis these defects may affect the formation of active centers (ions, radicals), destruction and cross-linking of macromolecules, and radiative gas release [6]. Therefore, the studies aimed at analyzing the radiolytic changes in the PTFE structure, which may directly affect the radiation-induced chemical processes in the polymer, are of particular importance.

In this paper, we report the results of studying the regularities and mechanisms of radiation-induced changes in the crystalline and amorphous phases in  $\gamma$ -irradiated powdered PTFE.

### EXPERIMENTAL

The objects of study were samples of powdered PTFE Ph4-D (GOST (State Standard) 14906-77). Weights of powdered PTFE (up to 10 g in mass) were placed in polyethylene packets and irradiated by  $\gamma$  quanta ( $^{60}\text{Co}$ ) in a nitrogen flow at room temperature

on the radioisotope system RKhM- $\gamma$ -20 (Mendeleev University of Chemical Technology, Moscow) to doses of 10–500 kGy with a fluence of  $1.5 \pm 0.3$  Gy/s.

The phase composition and crystal structure parameters of powdered PTFE were investigated at room temperature by X-ray diffraction (XRD) using a DRON-3M diffractometer ( $\text{CuK}\alpha$  radiation with a characteristic wavelength of 1.5406 Å, diffraction angle scanning range  $\theta = 5^\circ\text{--}80^\circ$ , scanning step  $0.05^\circ\text{--}0.02^\circ$ , exposure 1–20 s). The contents of the amorphous ( $X_a$ ) and crystalline ( $X_c$ ) phases were determined from the formula [7]

$$\frac{X_c}{X_a} = 1.8 \frac{A_c}{A_a}, \quad (1)$$

where  $A_c$  and  $A_a$  are, respectively, the areas under the peaks and amorphous halos observed in PTFE diffraction patterns and 1.8 is the Ruland factor [7]. The DOC value for PTFE was calculated using the relation

$$X_c [\%] = 100 - 100 / (1 + X_c / X_a). \quad (2)$$

At 19–30°C the repeating unit of the PTFE main chain is a slightly untwisted spiral, consisting of 7 turns and 15  $\text{CF}_2$  groups, which form a hexagonal packing with lattice constants  $a = 5.65$  Å and  $c = 19.50$  Å, sp. gr.  $P6mm$  [1, 2, 8]. Therefore, when indexing PTFE diffraction patterns, the quadratic forms for each peak in the diffraction pattern were calculated

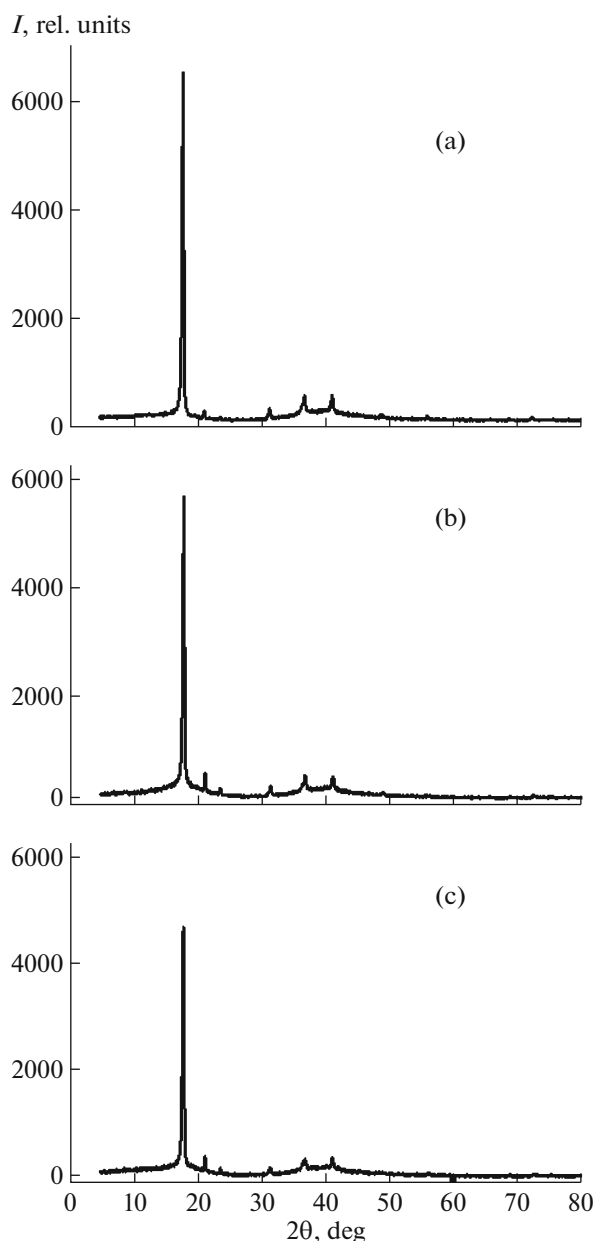


**Fig. 1.** X-ray diffraction patterns of powdered PTFE,  $\gamma$ -irradiated to doses of (a) 10, (b) 50, and (c) 500 kGy.

according to [3–5], using the formula for determining the Miller indices  $h, k, l$  in the hexagonal system. The interplanar spacing  $d_{hkl}$  was calculated from the Bragg formula [3–5]:

$$\frac{d_{hkl}}{n} = \frac{\lambda}{2 \sin \theta}, \quad (3)$$

where  $n$  is the diffraction peak order;  $n = 1$  within the kinetic approximation [5]. Then we calculated the ratio of the quadratic forms of each reflection to the quadratic form estimated for the first peak of the diffraction pattern ( $N$ ) and determined the Miller indices.

The DOC of the initial and irradiated PTFE powders was also determined by differential scanning calorimetry (DSC). Measurements were performed with a heat flow calorimeter DSC 204 F1 Phoenix. The DOC value was found from the formula

$$\text{DOC} = (\Delta H_{\text{melt exp}} / \Delta H_{\text{melt eq}}) \times 100\%, \quad (4)$$

where  $\Delta H_{\text{melt exp}}$  is the heat of fusion found from the thermograms and  $\Delta H_{\text{melt eq}}$  is the equilibrium heat of fusion for PTFE with  $\text{DOC} = 100\%$ , which amounted to 82 kJ/kg [9].

The measurement results were processed using the instrumental software. The recorded amorphous halos and crystalline peaks were approximated by Gaussians and Lorentzians, respectively.

## RESULTS AND DISCUSSION

The diffraction patterns of the PTFE powders irradiated to doses of 10–500 kGy (Fig. 1) contain identical sets of peaks (Table 1) and three amorphous halos in the ranges of  $2\theta = 10^\circ\text{--}25^\circ$  (maximum at  $2\theta = 14.70^\circ \pm 0.09^\circ$ );  $30^\circ\text{--}60^\circ$  ( $40.34^\circ \pm 0.07^\circ$ ), and  $70^\circ\text{--}80^\circ$  ( $75.40^\circ \pm 0.03^\circ$ ). The nature of these halos may be related to, respectively, intermolecular, intramolecular, and interatomic scattering in PTFE [10].

As an example, we will consider the results of indexing the diffraction pattern of PTFE powder  $\gamma$ -irradiated to a dose of 10 kGy. It is known [3–5] that the ratio of quadratic forms (or squared interplanar spacings) for the hexagonal system should not be obligatory integer. Only in particular cases, for the  $(hk0)$ - or  $(00l)$ -type planes, the parameter  $N$  is an integer that can take values  $N = 1, 3, 4, 7, 9, 12, 13$ , or 16, which correspond to peaks 1, 4, 5, 8, 9, 10, 11, and 13 in the diffraction patterns (Table 1). Additionally taking into account that  $N = 1, 4, 9$ , or 16 for the  $(00l)$  planes, one can identify peaks 1, 5, 9, and 13 as reflections 100, 200, 300, and 400, respectively.

Further identification on the crystalline peaks in the diffraction pattern was performed using the data of [8, 11–13]. As follows from Table 1, the combination of peaks 110, 200, 107, and 108 indicates that the crystalline phase has a hexagonal lattice and that the 15/7 conformation is present for the repeating unit of polymer chain in the PTFE powders under study [8]. The diffraction patterns of powdered PTFE irradiated to higher doses were indexed in the same way.

We could not determine the nature of the diffraction peak at  $2\theta = 21.362^\circ \pm 0.005^\circ$ . Note that it was reported previously [14] about the detection of a diffraction maximum of unknown origin at  $2\theta = 22^\circ$  in the diffraction patterns of PTFE subjected to explosive processing. Possibly, this reflection indicates the existence of several lattice types in the PTFE powders under study, which are due to the specific features of synthesis, aging, and radiative destruction of polymer [15].

**Table 1.** Indexing of the diffraction pattern of powdered PTFE  $\gamma$ -irradiated to a dose of 10 kGy in air at room temperature

Diffraction pattern	$2\theta$ , deg	$\sin\theta$	$d_{hkl}$ , Å	$(\sin\theta)^2$	$N$	$h$	$k$	$l$
1	$18.021 \pm 0.002$	0.15662	4.918	0.02453	0.99997	1	0	0
2	$21.362 \pm 0.005$	0.18534	4.156	0.03435	1.40034			
3	$23.789 \pm 0.130$	0.20611	3.737	0.04248	1.73187	0	1	3
4	$31.542 \pm 0.009$	0.27179	2.834	0.07387	3.01147	1	1	0
5*	$36.920 \pm 0.008$	0.31665	2.433	0.10026	4.08744	2	0	0
6					4.08744	1	0	7
7	$41.297 \pm 0.007$	0.35263	2.184	0.12435	5.06927	1	0	8
8	$49.077 \pm 0.034$	0.4153	1.855	0.17248	7.03128	2	1	0
9	$56.176 \pm 0.012$	0.47083	1.636	0.22168	9.03713	3	0	0
10	$65.887 \pm 0.028$	0.54382	1.416	0.29573	12.05605	2	2	0
11	$69.086 \pm 0.025$	0.56702	1.359	0.32151	13.10694	3	1	0
12	$72.650 \pm 0.009$	0.59236	1.300	0.3509	14.30478	0	0	15
13	$78.221 \pm 0.0119$	0.63082	1.221	0.39793	16.22233	4	0	0

\* Peak 200 manifests itself in the diffraction pattern as a shoulder of peak 107. The contribution of peak 200 could not be selected when approximating experimental data because of the high noise level.

It was established that the positions of all diffraction maxima observed in the diffraction patterns of PTFE irradiated to doses of 10–500 kGy, except for the first peak at  $2\theta = 18.021^\circ \pm 0.002^\circ$  and amorphous halos in the ranges of  $10^\circ$ – $25^\circ$  and  $30^\circ$ – $60^\circ$ , are barely sensitive to ionizing radiation.

As follows from Fig. 1, peak 100 dominates in the diffraction patterns of the PTFE  $\gamma$ -irradiated to doses of 10–500 kGy. With an increase in dose, peak 100 becomes weaker and wider, and its maximum shifts to larger (at doses close to 50 kGy) or smaller (at higher doses) diffraction angles  $2\theta$  (Figs. 2a, 2b, 3a).

The radiation-induced change in the profile of peak 100 may be related to its doublet nature (Fig. 2c). For the PTFE samples irradiated to doses of 10–500 kGy, the peak profile can be approximated by two Lorentzians with maxima in the ranges of  $17.87^\circ$ – $17.93^\circ$  and  $17.97^\circ$ – $18.03^\circ$ , depending on the dose absorbed (Fig. 3a). The identical dose dependences of the diffraction angles  $2\theta$  for the maxima of the components of peak 100 (Fig. 3a) suggest that the components at  $17.87^\circ$ – $17.93^\circ$  and  $17.97^\circ$ – $18.03^\circ$  may be due to the scattering centers that correspond to the hexagonal phase but are characterized by different interplanar spacings. Therefore, one can suggest existence of two types of crystallites in the PTFE studied (which are referred to below as crystals **1** (Cr1) and **2** (Cr2), respectively).

An analysis of the dose dependence of the Cr1 and Cr2 contents in PTFE, which was estimated from the

areas under the Lorentzian peaks (Fig. 3b), revealed a difference in the Cr1 and Cr2 sensitivities to ionizing radiation. In particular, the Cr1 content increased in the initial irradiation stage (at doses below 100 kGy) and started decreasing only when the dose reached 500 kGy (Fig. 3b, curve 1). In contrast, the Cr2 content monotonically decreased in the entire dose range (Fig. 3b, curve 2). The revealed processes occurred against the background of total decrease in the 100 reflection intensity.

Then one may suggest that the radiative destruction of Cr2 occurs over two possible mechanisms: some part of Cr2 is transformed into Cr1, and the other part is destroyed. The dose dependences of the contributions of the amorphous halos at  $10^\circ$ – $25^\circ$  and  $30^\circ$ – $60^\circ$  to the diffraction patterns of the PTFE powders under study (Fig. 3c; curves 1, 2), which were estimated from the area under the approximating Gaussian peak, are in favor of this suggestion. A tendency to decrease in the area under the halos was revealed in the initial irradiation stage (at doses below 50 kGy). However, a further increase in dose increases the area under the amorphous halo at  $10^\circ$ – $25^\circ$ , whereas the area under the halo at  $30^\circ$ – $60^\circ$  barely changes (Fig. 3c). No significant dose dependence was found for the area under the halo at  $70^\circ$ – $80^\circ$ . One may suggest that the contribution of the halo at  $10^\circ$ – $25^\circ$  increases as a result of radiative degradation of Cr2. The amorphous halo at  $30^\circ$ – $60^\circ$  is related to neither Cr1 nor Cr2, as is evidenced by its low sensitivity to  $\gamma$  radiation.

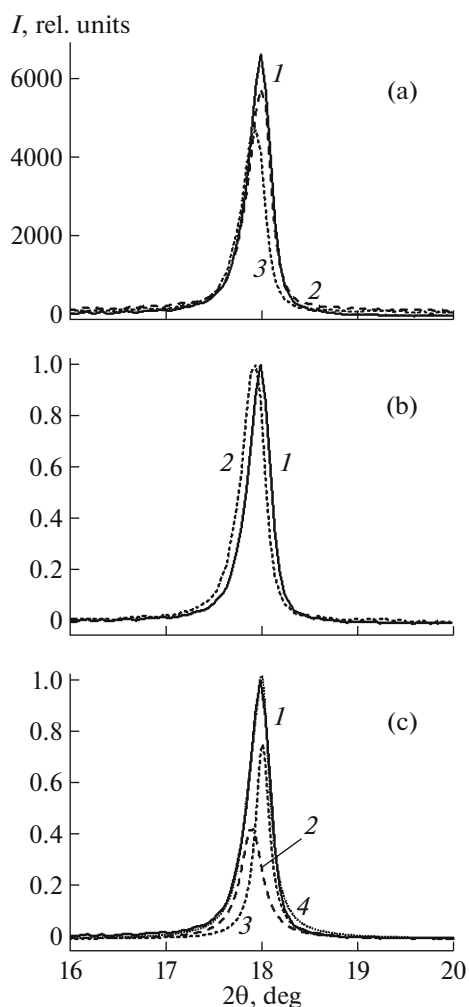


**Fig. 2.** Fragments of X-ray diffraction patterns in the vicinity of peak 100 for  $\gamma$ -irradiated powdered PTFE. (a) Irradiation to doses of (1) 10, (2) 50, and (3) 500 kGy. (b) Changes in the shape of peak 100 after irradiation to doses of (1) 10 and (2) 500 kGy. (c) Approximation of the profile of reflection 100 (irradiation to 10 kGy) by two Lorentzians: (1) experimental data; (2, 3) Cr1 and Cr2 components, respectively; and (4) calculated profile.

The dose dependences of the change in the interplanar spacings in Cr1 and Cr2, calculated from formula (2), have identical character (Fig. 4a). Therefore, lattice “compression” and decrease in interplanar spacing occur in both Cr1 and Cr2 in the initial irradiation stage. However, at doses above 50 kGy the radiation-induced deformation of Cr1 and Cr2 changes towards an increase in the interplanar spacing; i.e., the lattice “expands.”

Let us estimate the amplitude of the radiation-induced stress in PTFE [16] from the formula

$$\sigma = \frac{E}{\nu} \left| \frac{\Delta d}{d_0} \right|, \quad (5)$$

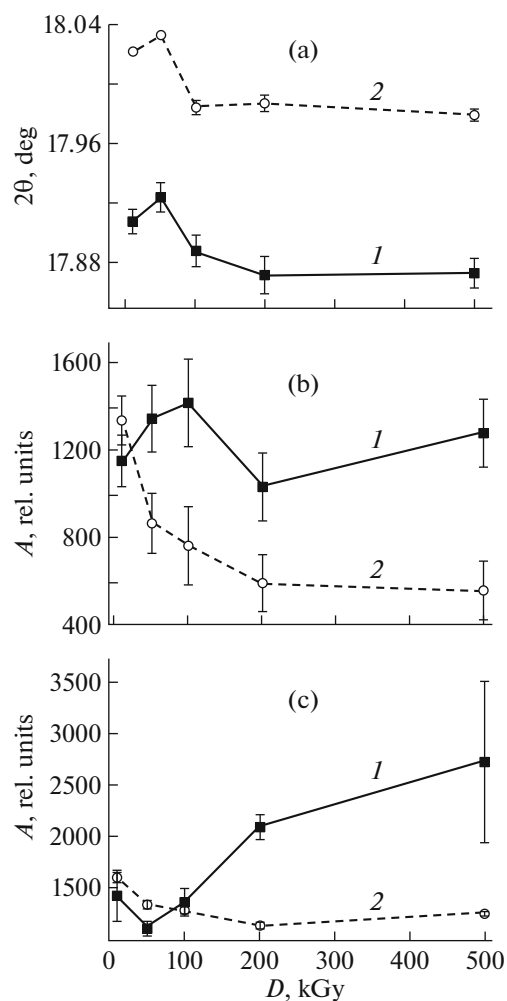


**Fig. 3.** Dose dependences of the (a) peak positions and (b) areas under the (1) Cr1 and (2) Cr2 components of the doublet line 100 and (c) amorphous halos at  $2\theta = (1) 10^\circ - 25^\circ$  and (2)  $30^\circ - 60^\circ$  in the diffraction patterns of  $\gamma$ -irradiated powdered PTFE.

where  $\sigma$  is the amplitude of the arising stress [MPa];  $E$  is Young’s modulus ( $E = 660$  MPa for PTFE [17]);  $\nu$  is the Poisson ratio (0.4–0.45 in the case of PTFE [18]);  $d_0$  [Å] are the initial interplanar spacings in Cr1 and Cr2, which were assumed to be equal to those for the PTFE irradiated to a dose 10 kGy (Fig. 4a); and  $\Delta d = |d - d_0|$  [Å] is the change in the interplanar spacing for the PTFE samples irradiated to doses above 10 kGy.

The dose dependences of the stresses developing in Cr1 and Cr2 under ionizing radiation are almost identical (Fig. 4b, curves 1, 2). Noteworthy is the change in the sign of radiation-induced stress occurring in the dose range of 50–100 kGy. It may indicate onset of crack formation and destruction of crystals of both types. Further increase in the irradiation dose is accompanied by a rise in the tensile stress, which stimulates even more the processes of radiative degrada-

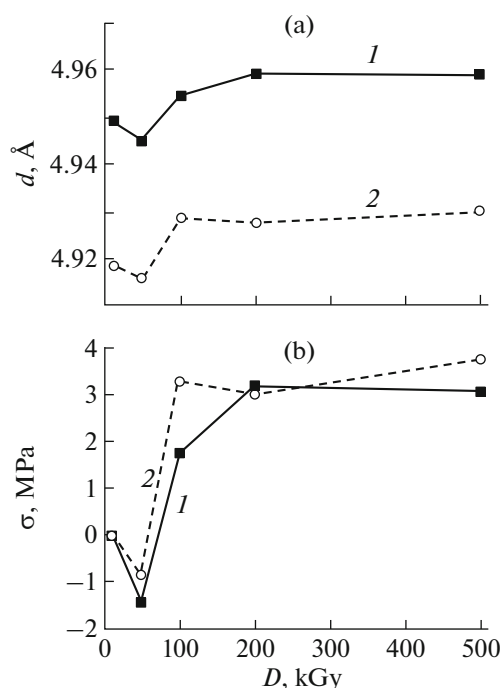


**Fig. 4.** Dose dependences of the (a) interplanar spacing and (b) amplitude of radiation-induced stress in  $\gamma$ -irradiated powdered PTFE.

tion of Cr1 and Cr2. It is likely that the ultimate tensile strength for Cr2 is lower than for Cr1, as a result of which Cr2 is more intensively destroyed during irradiation. The occurrence of a topochemical reaction of Cr2 transformation into Cr1 in only the initial stage of PTFE radiolysis (Fig. 3b) may indicate the existence of certain conditions necessary for implementing this process, which can be related to the polymer chain length [1, 2].

DSC measurements revealed a significant increase in the DOC of powdered PTFE in the initial stage of  $\gamma$  irradiation: DOC = 34% in the unirradiated PTFE,

**Table 2.** DOCs of  $\gamma$ -irradiated powdered PTFE, calculated based on DSC and XRD data, for different absorbed doses

Dose, kGy	DOC <sub>DSC</sub> , %	DOC <sub>XRD</sub> , %
0	34.0	—
10	62.82	81.46
50	80.62	81.69
100	79.0	83.20
200	79.0	85.54
500	77.81	86.73
1000	79.78	

whereas the DOC in the PTFE samples irradiated to 50 kGy increased to 80.6% and only slightly decreased in the dose range of 100–500 kGy. This change in DOC with a change in the irradiation dose is consistent with the data of [1]. However, an inconsistency between the DSC and XRD estimates of radiation-induced change in DOC was previously noted in [6].

It was found that the best agreement between the DOC estimates by both methods can be obtained by evaluating the ratio of the sum of areas under the peaks corresponding to Cr1 and Cr2 and the halo at  $10^\circ$ – $25^\circ$  to the area under the halo at  $30^\circ$ – $60^\circ$  using formulas (1) and (2) (Table 2). Hence, the nature of the halo at  $10^\circ$ – $25^\circ$  is related to the scattering from fragments of destructured Cr1 and Cr2, which are likely localized at the interface between the amorphous and crystalline PTFE phases.

## CONCLUSIONS

It was found that the radiation-induced change in the PTFE crystallinity is a complex phenomenon, caused by the destruction processes and topochemical reactions. The morphology of polymer crystals, which is determined by the PTFE synthesis conditions, may play an important role in these processes [1]. The formation of radiation-induced stresses during PTFE irradiation was revealed for the first time, and their role in the radiolytic transformations of the crystalline PTFE phase was demonstrated. Note that the consideration of the specific features of PTFE radiolysis found in this study allows one to obtain XRD estimates of the PTFE DOC comparable with the DSC data on the same samples.

The results of studying the morphology of crystals in powdered PTFE by transmission electron microscopy and full-profile analysis of peak 100 [5] will be reported in the next papers.

## FUNDING

This study was supported by the Russian Foundation for Basic Research, project no. 17-07-00524.

## REFERENCES

1. Yu. A. Panshin, S. G. Malkevich, and Ts. S. Dunaevskaya, *Teflon* (Khimiya, Leningrad, 1978) [in Russian].
2. B. Wunderlich, *Macromolecular Physics*, Vol. 2 (Academic, New York, 1976).
3. Yu. K. Egorov-Tismenko, *Crystallography and Crystal Chemistry: A Textbook*, Ed. by V. S. Urusov (KDU, Moscow, 2005) [in Russian].
4. Ya. S. Umanskii, Yu. A. Skakov, A. N. Ivanov, and L. N. Rastorguev, *Crystallography, X-Ray Diffraction, and Electron Microscopy* (Metallurgiya, Moscow, 1982) [in Russian].

5. A. A. Klopotov, Yu. A. Abzaev, A. I. Potekaev, et al., *Fundamentals of X-Ray Diffraction Analysis in Materials Science* (Izd-vo TGASU, Tomsk, 2012) [in Russian].
6. V. K. Milinchuk, E. R. Klinshpont, and V. I. Tupikov, *Fundamentals of Radiation Resistance of Organic Materials* (Energoatomizdat, Moscow, 1994) [in Russian].
7. P. J. Raea and D. M. Dattelbaum, *Polymer* **45**, 7615 (2004).
8. V. M. Bouznik, S. D. Kirik, L. A. Solovyov, et al., *Powder Diffraction* **19**, 135 (2004).
9. S.-F. Lau, H. Suzuki, and B. Wunderlich, *J. Polym. Sci. Polym. Phys. Ed.* **22**, 379 (1984).
10. V. M. Polikarpov, S. I. Lazarev, Yu. M. Golovin, et al., *Vestn. TGU* **20**, 910 (2015).
11. Yu. A. Lebedev, Yu. M. Korolev, A. V. Rebrov, et al., *Crystallogr. Rep.* **55** (4), 615 (2010).
12. Yu. A. Lebedev, Yu. M. Korolev, V. M. Polikarpov, et al., *Crystallogr. Rep.* **55** (4), 609 (2010).
13. Yu. E. Vopilov, L. N. Nikitin, G. Yu. Yurkov, et al., *J. Supercrit. Fluids* **62**, 204 (2012).
14. L. N. Ignat'eva, N. A. Adamenko, G. V. Agafonova, et al., *Vestn. DVO Ross. Akad. Nauk*, No. **5**, 44 (2013).
15. J. Zhang, Y. Guo, J. Z. Xu, et al., *Appl. Phys. Lett.* **86**, 131501 (2005).  
<https://doi.org/10.1063/1.1894598>
16. E. A. Barbashev, V. A. Bogatov, V. I. Kozin, et al., *Fiz.-Khim. Mekh. Mater.* **21**, 74 (1985).
17. A. Ya. Gol'dman, *Strength of Construction Plastics* (Mashinostroenie, Leningrad, 1979) [in Russian].
18. S. B. Ainbinder, E. M. Tyunina, and K. I. Tsirule, *Properties of Polymers in Different Strained States* (Khimiya, Moscow, 1981) [in Russian].

*Translated by Yu. Sin'kov*